Heliyon 9 (2023) e22186

Contents lists available at ScienceDirect

Heliyon

journal homepage: www.cell.com/heliyon

Moutai Distiller's grains Polyphenol extracts and rutin alleviate DSS-induced colitis in mice: Modulation of gut microbiota and intestinal barrier function (R2)

Jin-hu Chen [a], Cai-li Zhao [a], Yong-su Li [b,c], Yu-bo Yang [b,c], Jian-guang Luo [a,**], Chao Zhang [a,*], Li Wang [c,d,***]

[a] *Jiangsu Key Laboratory of Bioactive Natural Product Research and State Key Laboratory of Natural Medicines, School of Traditional Chinese Pharmacy, China Pharmaceutical University, Nanjing 211198, China*
[b] *Kweichow Moutai Co., Ltd, Zunyi, Guizhou 564501, China*
[c] *Baijiu manufacturing innovation center of Guizhou Province, Zunyi, Guizhou 564501, China*
[d] *Kweichow Moutai Group, Zunyi, Guizhou 564501, China*

ARTICLE INFO

Keywords:
Moutai distiller's grains
Distiller's grains polyphenol
Gut microbiota
Intestinal mucosal barrier

ABSTRACT

Distiller's grains, byproducts of the brewing process, represent a valuable resource for extracting natural phenolic compounds due to their significant global production. This study presents the first evidence of the protective effects of Moutai distiller's grain polyphenol extract (MDGP) on dextran sulfate sodium (DSS)-induced colitis in mice. These protective effects manifest predominantly through the amelioration of general colitis indices and histopathological improvements. Utilizing liquid chromatography-high-resolution electrospray ionization mass spectrometry (LC-HR-ESI-MS), the main components of MDGP were identified as rutin, quercetin, naringenin, and dihydroquercetin. Moreover, a novel mechanism was elucidated by which rutin, the primary active component of MDGP, alleviates DSS-induced colitis. Assessment of intestinal barrier function, microbial sequencing, fecal transplantation, and antibiotic depletion experiments revealed that rutin suppresses the abundance of pathogenic bacteria (*Helicobacter*, *Klebsiella*, and *Veillonella*) while promoting the proliferation of beneficial bacteria (*Ruminococcus_torques_group*, *Lachnoclostridium*, and *norank_f_Muribaculaceae*). This modulation culminates in elevated butyric acid concentrations within short-chain fatty acids (SCFAs), amplified integrity of tight (ZO-1, occludin) and adherent (E-cadherin, β-catenin) junctional complexes, fortified intestinal barrier function, and diminished intestinal inflammation.This investigation accentuates the innovative therapeutic potential of MDGP and its main active component, rutin, in assuaging DSS-induced intestinal inflammation and fortifying the intestinal barrier through a mechanism predominantly mediated by the intestinal microbiota. Such insights potentially elevate the prominence of distiller's grains in the realm of functional food development.

* Corresponding author. Longmian Street 639, Nanjing, Jiangsu 211198, China.
** Corresponding author. Kweichow Moutai Co., Ltd, Zunyi, Guizhou 564501, China.
*** Corresponding author. Baijiu manufacturing innovation center of Guizhou Province, Zunyi, Guizhou 564501, China.
E-mail addresses: luojg99@163.com (J.-g. Luo), zhangchao19860910@126.com, zhangchao@cpu.edu.cn (C. Zhang), 1178485794@qq.com (L. Wang).

https://doi.org/10.1016/j.heliyon.2023.e22186
Received 3 August 2023; Received in revised form 31 October 2023; Accepted 6 November 2023
Available online 11 November 2023

1. Introduction

Ulcerative colitis (UC), an idiopathic disease hallmarked by chronic colonic inflammation and ulceration that disturbs colon homeostasis and leads to significant epithelial damage, is increasingly prevalent worldwide, with a notable demographic shift toward younger individuals [[1,2]]. Despite the enigmatic etiology of UC, it is postulated that a multifaceted matrix of genetic susceptibility, environmental elements, immune malfunction, intestinal microbial imbalance, and compromised intestinal mucosal barrier function converge in disease manifestation [[3]]. Traditional anti-inflammatory drugs, typified by mesalazine (5-ASA), often come with demanding dosage protocols, an extensive array of side effects, and limited effectiveness in promoting mucosal recovery. Immune-centric therapies have expanded the treatment options for UC; however, issues related to drug resistance and non-specific effects continue to pose significant challenge [[4,5]]. Thus, there is an imperative need for more effective and safer therapeutic strategies to prevent and alleviate UC, with the ultimate goal of diminishing the reliance on long-term medications and the recurrence of disease exacerbations in patients.

The intestinal mucosal barrier and gut microbiota are integral determinants of intestinal health [[6]]. In UC, gut microecological imbalance is typified by diminished diversity of gut flora, skewed bacterial phyla proportions, reduced beneficial metabolites (e.g., short-chain fatty acids (SCFA)), and elevated detrimental metabolites (e.g., lipopolysaccharides (LPS)) [[7,8]]. The intestinal mucosal barrier, formed by interconnected epithelial cells, serves as the primary defense against pathogenic bacteria and harmful substances [[9]]. In the context of UC, this barrier is compromised, with alterations in tight junction protein (TJ) and adherens junction protein (AJ) expression [[10]]. The disruption of TJs facilitates the pathogenic bacterial invasion from the lumen to the lamina propria, prompting an inflammatory response typified by the overproduction of proinflammatory cytokines (TNF-α, IL-1β, and IL-6), thereby exacerbating intestinal inflammation and epithelial damage [[11]]. Dietary polyphenols, abundant in diets high in natural components, have been linked to reduced mortality from several chronic diseases, such as cardiovascular disease, cancer, and diabetes, and their beneficial effects on intestinal health have been underscored in the realm of inflammatory bowel disease (IBD) prevention and treatment [[12–14]].

Distiller's grains, the primary residues of the brewing process, are recognized as a plentiful source of bioactive compounds (e.g., polyphenols, tannins, and anthocyanins) but present preservation challenges, potentially leading to environmental pollution and resource wastage [[15]]. Current applications, including organic fertilizer production, protein feed, edible fungus cultivation, and vinegar production, have yet to fully exploit the abundant resources of distiller's grains. Therefore, a detailed exploration of the nutritional constituents and functional substances within distiller grains is crucial for enhancing resource utilization in the brewing industry and fostering sustainable development. Phenolic compound recovery from these byproducts is an emerging and promising strategy within a circular economy framework [[16]]. However, existing studies have largely focused on lees derived from fruits, leaving a research gap in grain-based lees, such as those from sorghum, corn, and wheat. Moutai distiller's grains, produced primarily from sorghum and wheat, reportedly contain high concentrations of flavonoids and polyphenols. Despite this, the biological activities of Moutai distiller's grain polyphenol extracts (MDGP) remain underinvestigated.

The present study aimed to scrutinize the in vivo anti-UC potential of MDGP by employing a dextran sodium sulfate (DSS)-induced mouse colitis model. Furthermore, the active components of MDGP, including rutin, quercetin, naringenin, and dihydroquercetin, were characterized via HPLC-Q-TOF-MS/MS methodologies. Among these, rutin, a primary constituent in MDGP known for its therapeutic efficacy in acute and chronic colitis, merited further scrutiny. Importantly, rutin exhibits a benign toxicity profile and lacks oxidative properties, unlike aglycones (demonstrating mutagenic and cytotoxic effects) and other flavonoids (for instance, quercetin can behave as a pro-oxidant and catalyze oxygen radical production under certain circumstances), making it an ideal candidate for further exploration [[17]]. However, the bioavailability of rutin in vivo is restricted, and despite its known interactions with intestinal microbial communities, scant information exists regarding its influence on intestinal ecological imbalances in DSS-induced colitis [[18]]. Thus, the study proceeded to further examine the beneficial impacts and novel mechanisms of rutin, as the primary active constituent of MDGP, on DSS-induced colitis. Verification of its advantageous effect was accomplished through gut microbiome sequencing, fecal microbiota transplantation (FMT), and antibiotic depletion, demonstrating that rutin modulates SCFA production in a gut microbiota-dependent manner, rejuvenates intestinal mucosal barrier function, and mitigates intestinal inflammation.

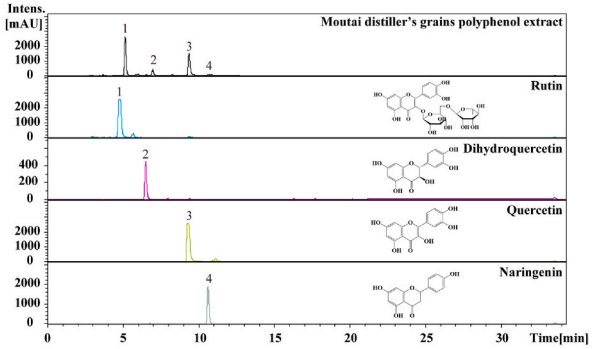

Fig. 1. Chemical composition analysis of Moutai Distiller's grain polyphenol extract.

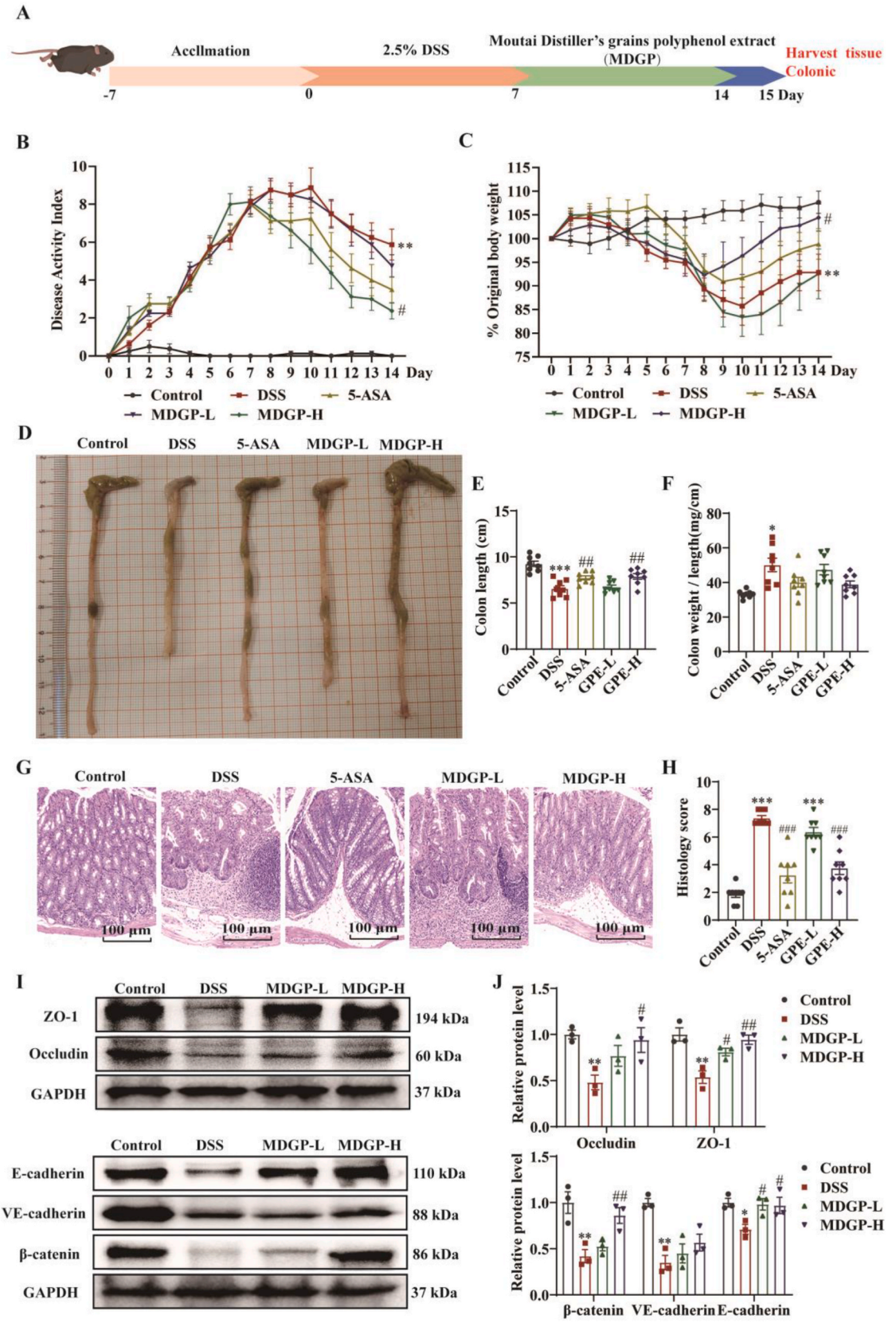
A
Acclimation
2.5% DSS
Moutai Distiller's grains polyphenol extract (MDGP)
Harvest tissue Colonic
-7
0
7
14
15 Day
B
Disease Activity Index
Day
Control
DSS
5-ASA
MDGP-L
MDGP-H
C
% Original body weight
Day
Control
DSS
5-ASA
MDGP-L
MDGP-H
D
Control
DSS
5-ASA
MDGP-L
MDGP-H
E
Colon length (cm)
Control
DSS
5-ASA
GPE-L
GPE-H
F
Colon weight / length(mg/cm)
Control
DSS
5-ASA
GPE-L
GPE-H
G
Control
DSS
5-ASA
MDGP-L
MDGP-H
100 μm
H
Histology score
Control
DSS
5-ASA
GPE-L
GPE-H
I
Control
DSS
MDGP-L
MDGP-H
ZO-1
194 kDa
Occludin
60 kDa
GAPDH
37 kDa
E-cadherin
110 kDa
VE-cadherin
88 kDa
β-catenin
86 kDa
GAPDH
37 kDa
J
Relative protein level
Occludin
ZO-1
Control
DSS
MDGP-L
MDGP-H
β-catenin
VE-cadherin
E-cadherin

Fig. 2. Moutai Distiller's grain polyphenol extracts improve colitis signs of DSS-induced colitis in mice. **(A)** Experimental design of rutin's effect on DSS-induced mice; (B) body weight change; **(C)** DAI score; **(D)** representative images of colons in each mouse group; **(E)** colon length; **(F)** colon weight/length ratio; **(G, H)** representative images of HE-stained colon tissue (scale bar, 100 μm) and histopathological scores for each group; **(I, J)** representative immunoblots and relative expression levels of AJ and TJ proteins. Data are expressed as the means ± SEMs ($^{*}P < 0.05$, $^{**}P < 0.01$, $^{***}P < 0.001$ vs Control group; $^{\#}P < 0.05$, $^{\#\#}P < 0.01$, $^{\#\#\#}P < 0.001$ vs DSS group), n = 8.

2. Results

2.1. Analysis of chemical composition in Moutai Distiller's grains Polyphenol extract

Utilizing a 70 % ethanol solution, polyphenols were extracted from Moutai Distiller's Grains. This extract underwent subsequent treatments with petroleum ether, ethyl acetate, and n-butanol. The ethyl acetate and n-butanol fractions were amalgamated and purified via a D101 macroporous adsorbent resin column, yielding the Moutai Distiller's Grains Polyphenol Extract (MDGP). An LC-HR-ESI-MS/MS technique was utilized to discern the chemical composition of MDGP(Fig. S1). Rutin, quercetin, naringenin, and dihydroquercetin emerged as the primary active constituents of the purified Moutai Distiller's Grains polyphenol extract (Fig. 1).

2.2. Moutai Distiller's grains Polyphenol extract alleviates DSS-induced colitis symptoms in mice

Ulcerative colitis typically manifests with clinical indicators such as weight loss, diarrhea, and bloody stools. We established an experimental colitis model through the administration of 2.5 % DSS (Fig. 2A). This DSS administration precipitated a significant

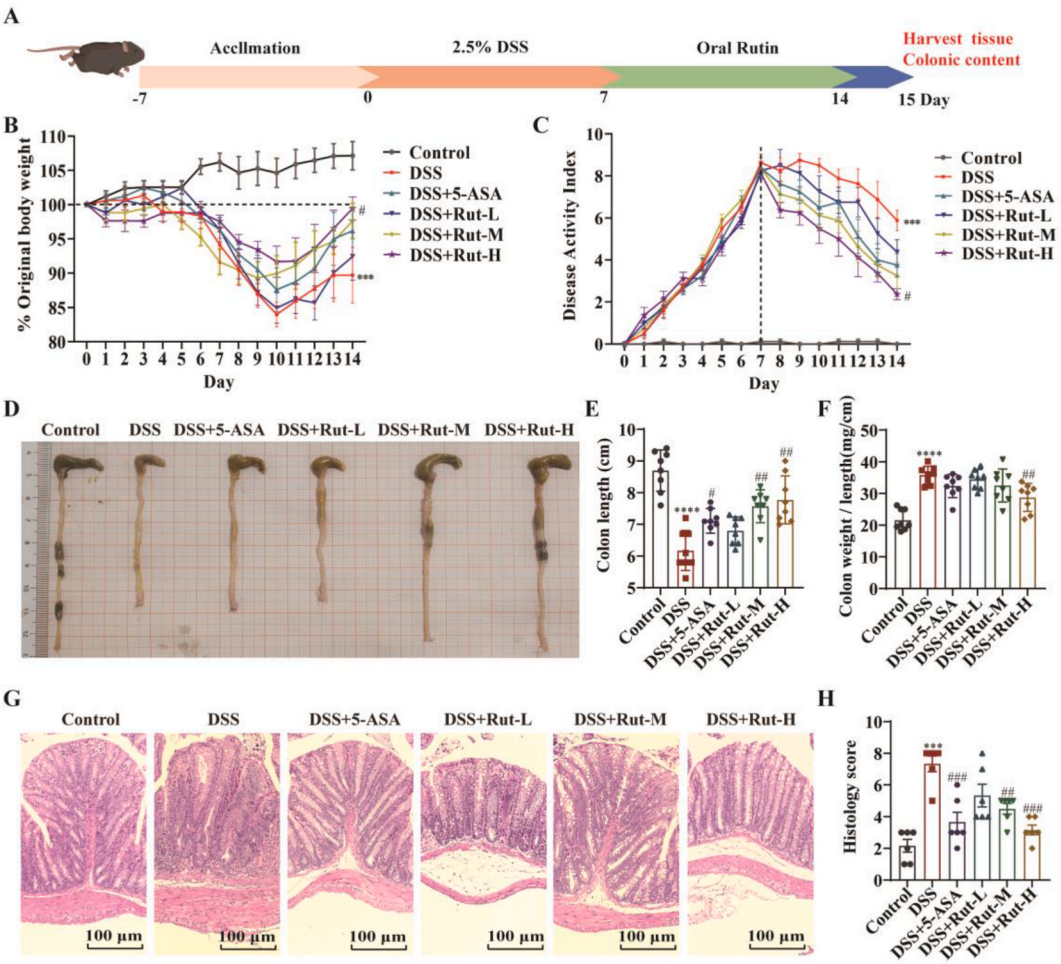

Fig. 3. Rutin ameliorates the pathological symptoms of DSS-induced colitis in mice. **(A)** Experimental design of rutin's effect on DSS-induced mice; **(B)** body weight change; **(C)** DAI score; **(D)** representative images of colons in each mouse group; **(E)** colon length; **(F)** colon weight/length ratio; **(G, H)** representative images of HE-stained colon tissue (scale bar, 100 μm) and histopathological scores for each group. Data are expressed as the means ± SEMs ($^{*}P < 0.05$, $^{**}P < 0.01$, $^{***}P < 0.001$ vs Control group; $^{\#}P < 0.05$, $^{\#\#}P < 0.01$, $^{\#\#\#}P < 0.001$ vs DSS group), n = 8.

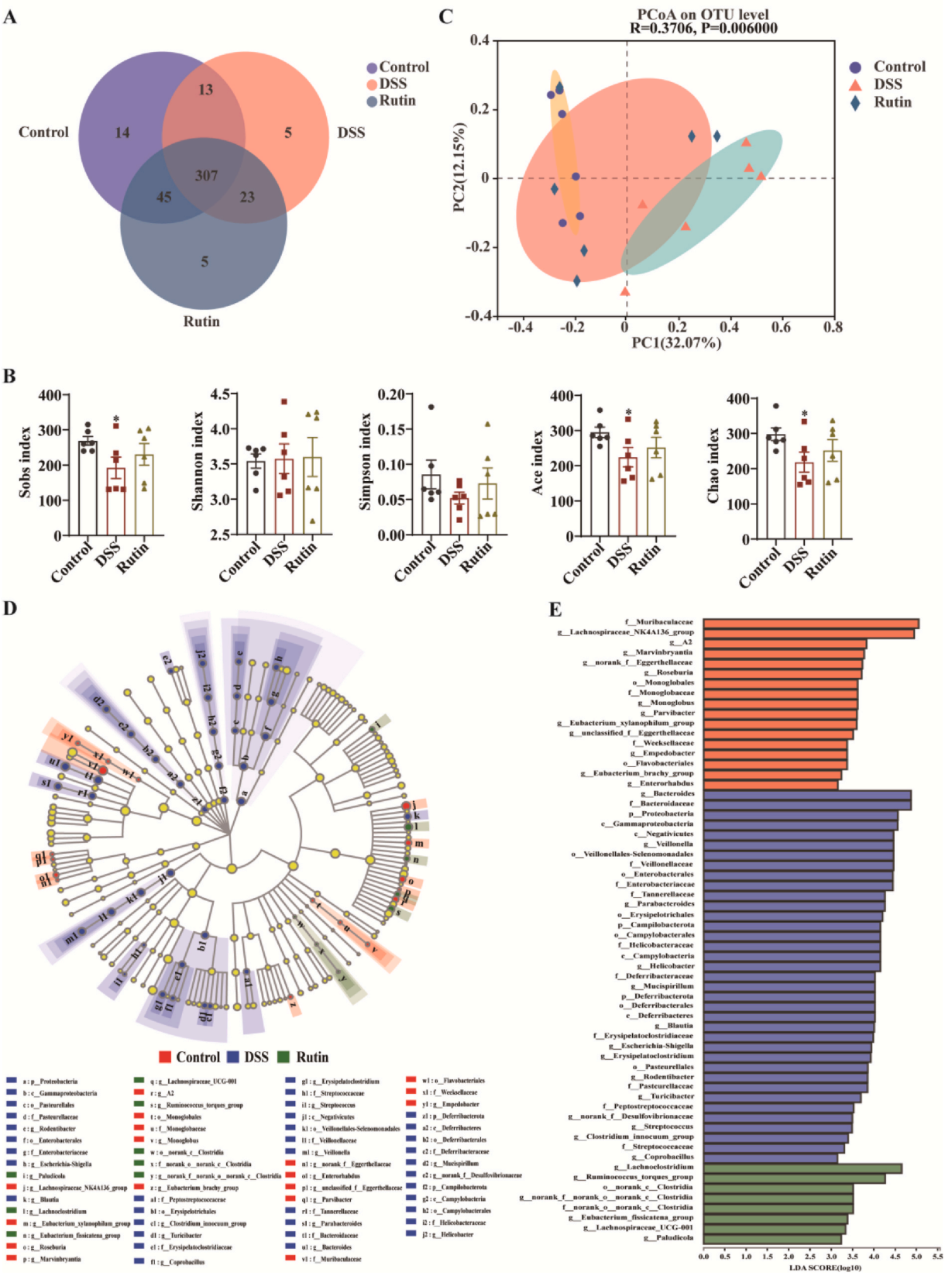

(caption on next page)

Fig. 4. Effect of rutin on intestinal microbial diversity and abundance in mice with DSS-induced colitis. **(A)** Venn diagram; **(B)** Alpha diversity analysis; **(C)** Multiple sample PCoA based on Bray–Curtis distance for OTU; **(D)** Cladogram illustrating the results of LEfSe analysis; **(E)** LDA scores for bacterial taxa significantly enriched in gut microbiota from each group (LDA score >3); Data are expressed as the means ± SEMs ($^{*}P < 0.05$, $^{**}P < 0.01$, $^{***}P < 0.001$ vs Control group; $^{\#}P < 0.05$, $^{\#\#}P < 0.01$, $^{\#\#\#}P < 0.001$ vs DSS group), n = 6.

escalation in DAI scores related to weight loss, fecal consistency, and occult blood in feces, validating successful colitis induction in mice. Treatments with varying doses of MDGP or 5-ASA resulted in improvements in these pathological features and DAI scores in DSS-induced mice (Fig. 2B and C). Mice in the DSS group exhibited a reduction in colonic length and an increased colon weight/length ratio compared to the control group. These symptoms were mitigated in UC mice following treatment with each dose group of MDGP and 5-ASA (Fig. 2D–F). Histopathological analysis highlighted that DSS-administered mice demonstrated widespread mucosal ulceration, inflammatory cell infiltration, crypt damage, and surface epithelial disruption, along with significantly heightened histopathological scores. Treatment with varying doses of MDGP and 5-ASA significantly ameliorated these symptoms (Fig. 2G and H). Moreover, protein immunoblotting results indicated a significant boost in the expression levels of TJ proteins (ZO-1, Occludin) and AJ proteins (E-cadherin, β-catenin) in the colonic tissues of mice with colitis following MDGP supplementation, thereby improving the intestinal mucosal barrier function (Fig. 2I and J). These findings indicate that MDGP may mitigate both the symptoms of colitis and colonic damage in mice subjected to DSS-induced colitis.

2.3. Rutin alleviates disease symptoms, histopathological features, and gut microbiota dysbiosis in DSS-induced colitis mice

Rutin, a key component of MDGP, has been shown to exhibit various bioactivities and potential therapeutic effects in colitis treatment, despite its poor bioavailability in vivo. Notably, the anti-UC mechanism of action of rutin and its clinical application value warrant further exploration [[19,20]]. Rutin, due to its inherent nontoxic and nonoxidizing properties, holds superior developmental potential and research value compared to aglycones (mutagenic and cytotoxic) and other flavonoids such as quercetin and myricetin, which act as pro-oxidants and foster oxygen radical production. Rutin administration alleviated symptoms of DSS-induced colitis, chiefly evidenced by a reduction in DAI scores, recuperation of weight, elongation of the colon, and a decline in the colon weight-to-length ratio (Fig. 3A–F). Further histological analysis showed that rutin administration curtailed DSS-induced inflammatory cell infiltration and damage to the colonic mucosa (Fig. 3G and H).

A wealth of evidence indicates a close association between gut microbial imbalance and the initiation of the intestinal mucosal inflammation cascade leading to colitis. The impact of rutin treatment on alterations in gut microbiota induced by DSS was evaluated through a 16S rDNA high-throughput sequencing assay of fecal bacteria. The interplay between OTUs and different treatment groups was depicted via Venn diagrams (Fig. 4A). With a similarity screening of 97 %, a total of 412 OTUs were derived, of which 307 OTUs were shared by the three groups. Remarkably, the rutin and control groups shared a significantly larger number of common OTUs than the DSS and control groups (45 vs 13), suggesting that rutin might partially rectify gut microbiota dysbiosis in colitis mice. Alpha-diversity analysis primarily gauged the community diversity and richness of the mycota. As illustrated in Fig. 4B, the Shannon and Simpson diversity indices did not display significant differences between the groups. In the DSS-treated group of mice, the Sobs, Chao, and Ace richness indices fell by 28.46 % ($P < 0.05$), 26.60 % ($P < 0.05$), and 23.99 % ($P < 0.05$), respectively, compared to the control group, while these indices in the intestinal tract of the rutin-treated group increased by 19.84 %, 15.32 %, and 12.26 %, respectively. Similar trends were discerned in β-diversity based on the Bray–Curtis distance of OTUs for PCoA (ANOSIM: $R = 0.371$, $P = 0.006$, Fig. 4C), indicating that DSS significantly disrupted the gut microbiota, whereas rutin moderated it. LefSe analysis was employed to pinpoint genera with significant differences, with LDA values over 4 serving as the screening criteria for dominant microorganisms. The results revealed a marked enrichment of pathogenic bacteria such as *Bacteroides*, *Bacteroidaceae*, *Gammaproteobacteria*, and *Enterobacteriaceae* in the DSS group. Conversely, a higher proportion of beneficial bacteria, such as *Ruminococcus* and *Lachnoclostridium*, was observed in the rutin group (Fig. 4D and E).

To further elucidate the influence of rutin on the structure of the intestinal microbiota, the composition and relative abundance of intestinal microorganisms were analyzed at the phylum, family, and genus levels. At the phylum level, *Firmicutes* and *Bacteroidetes* emerged as the two predominant phyla, accounting for over 80 % of the total content (Fig. 5A). Intriguingly, DSS treatment significantly amplified the levels of *Proteobacteria* and *Campilobacterota*, whereas rutin treatment noticeably diminished them (Fig. 5B). At the family level, detrimental bacterial families such as *Bacteroidaceae*, *Enterobacteriaceae*, *Erysipelatoclostridiaceae*, *Helicobacteraceae*, and *Veillonellaceae* showed a significant increase post DSS treatment. In contrast, rutin treatment led to a significant reduction in harmful bacterial families such as *Enterobacteriaceae*, *Veillonellaceae, and Helicobacteraceae*, while a significant increase was observed in the beneficial bacterial family *Muribaculaceae* (Fig. 5C and D). At the genus level, harmful bacterial genera, including *Bacteroides*, *Helicobacter*, *Klebsiella*, and *Veillonella*, significantly increased after DSS treatment, while the beneficial bacterial genus *Lachnospiraceae_NK4A136_group* significantly decreased. Upon rutin treatment, the levels of harmful bacterial genera, including *Helicobacter*, *Klebsiella*, *Veillonella*, and *Blautia,* significantly decreased, whereas the beneficial bacterial genus *norank_f_Muribaculaceae* markedly increased (Fig. 5E–G). These findings highlight the promising role of rutin in modulating gut microbiota composition, potentially contributing to its therapeutic effects in mitigating colitis symptoms.

2.4. Rutin reestablishes intestinal SCFA production in DSS-induced colitis mice

SCFAs serve as a vital energy supply for intestinal epithelial cells and contribute to the maintenance of intestinal function and the

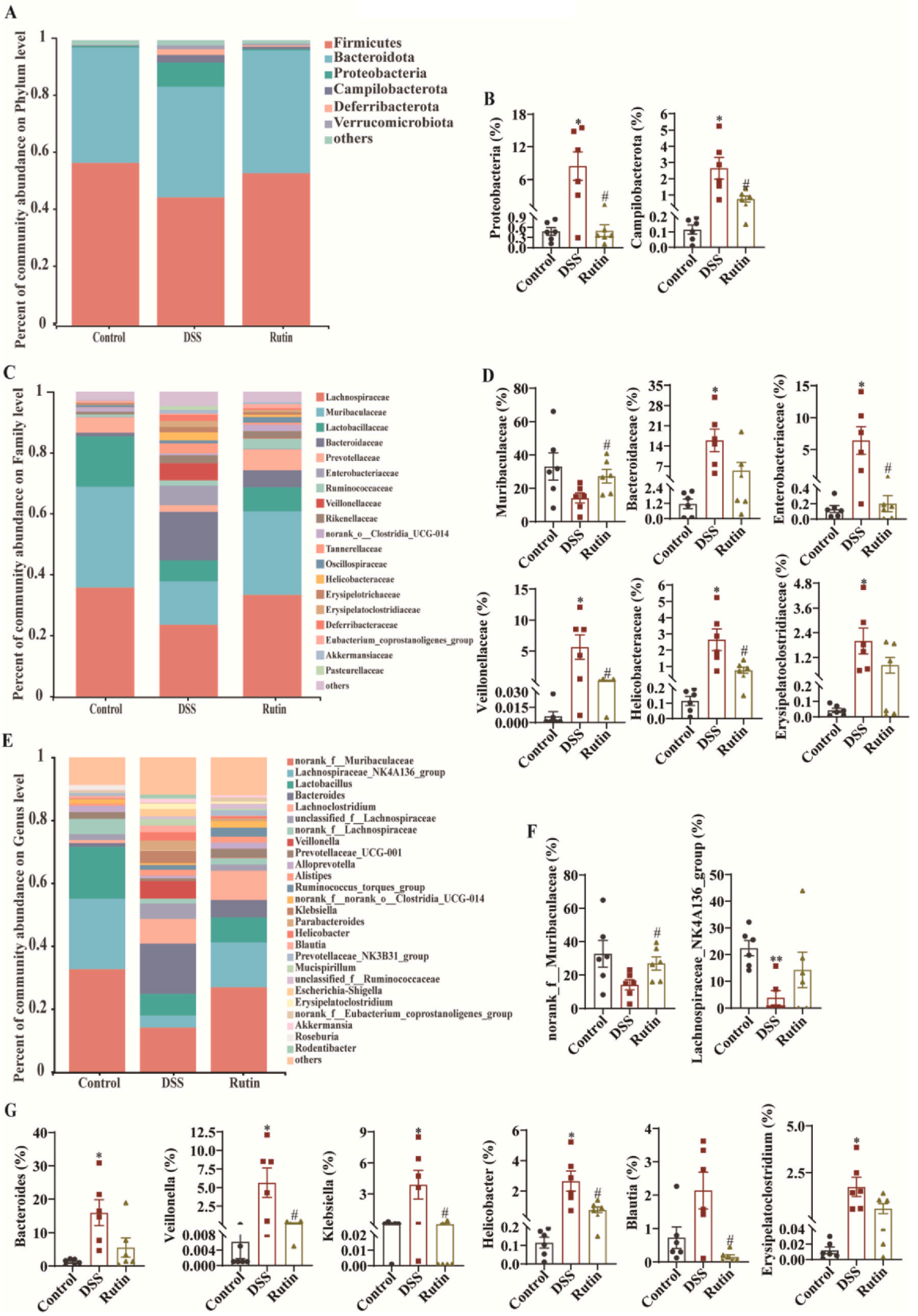

(caption on next page)

Fig. 5. Effect of rutin on the composition of the intestinal microbial community in mice with DSS-induced colitis. **(A)** Relative abundance of gut microbiota at the phylum level; **(B)** Relative abundance of bacteria significantly altered at the phylum level; **(C)** Relative abundance of gut microbiota at the family level; **(D)** Relative abundance of bacteria significantly altered at the family level; **(E)** Relative abundance of gut microbiota at the genus level; **(F, G)** Relative abundance of bacteria significantly altered at the genus level. Data are expressed as the means ± SEMs ($^{*}P < 0.05$, $^{**}P < 0.01$, $^{***}P < 0.001$ vs Control group; $^{\#}P < 0.05$, $^{\#\#}P < 0.01$, $^{\#\#\#}P < 0.001$ vs DSS group), n = 6.

structure and function of epithelial cells, a process crucial for intestinal health [[21]]. IBD patients and experimental colitis models exhibit disrupted SCFA levels [[22]]. The most prominent intestinal SCFAs encompass acetic acid, propionic acid, and butyric acid, while isobutyric acid, valeric acid, isovaleric acid, and capric acid are present in lesser quantities. Analysis via GC−MS indicated that in comparison to the control group, the DSS group had significantly lower levels of butyric acid, isobutyric acid, valeric acid, isovaleric acid, and capric acid, without significantly impacting acetic acid and propionic acid levels. Rutin treatment notably elevated the levels of butyric acid in comparison to the DSS group (Fig. 6A–G).

2.5. Rutin modulates inflammatory cytokine balance in DSS-induced colitis mice

The use of rutin supplementation led to an increase in the abundance of the beneficial bacteria *Lachnoclostridium* and a subsequent rise in its metabolite, butyric acid, within the mouse intestine, potentially contributing to an anti-inflammatory effect. The influence of rutin on the intestinal inflammatory response was further explored by measuring the levels of MPO and LPS within colonic tissues, as well as the levels of various inflammatory cytokines. MPO, an enzyme predominantly located in neutrophils, serves as a quantitative marker of colonic mucosa inflammation and neutrophil infiltration [[23]]. LPS is an endotoxin produced by pathogenic bacteria and is an important indicator of intestinal permeability [[24,25]]. As Fig. 7A and B illustrate, the DSS group showed significantly elevated levels of MPO and LPS compared to the control group, with rutin supplementation mitigating this increase, implying that rutin curtailed the infiltration of inflammatory cells into the colon and alleviated active intestinal inflammation. Fig. 7C–I highlight that the DSS group displayed significantly increased levels of proinflammatory cytokines such as TNF-α, IL-1β, IL-6, TGF-β, IL-17A, and IL-18 in the colonic tissue compared to the control group, while the levels of the anti-inflammatory cytokine IL-10 significantly decreased. Rutin treatment effectively reversed this inflammatory response, indicating that rutin plays a significant role in modulating the expression of intestinal inflammatory cytokines in colitis mice, contributing to the management of inflammation and maintenance of intestinal

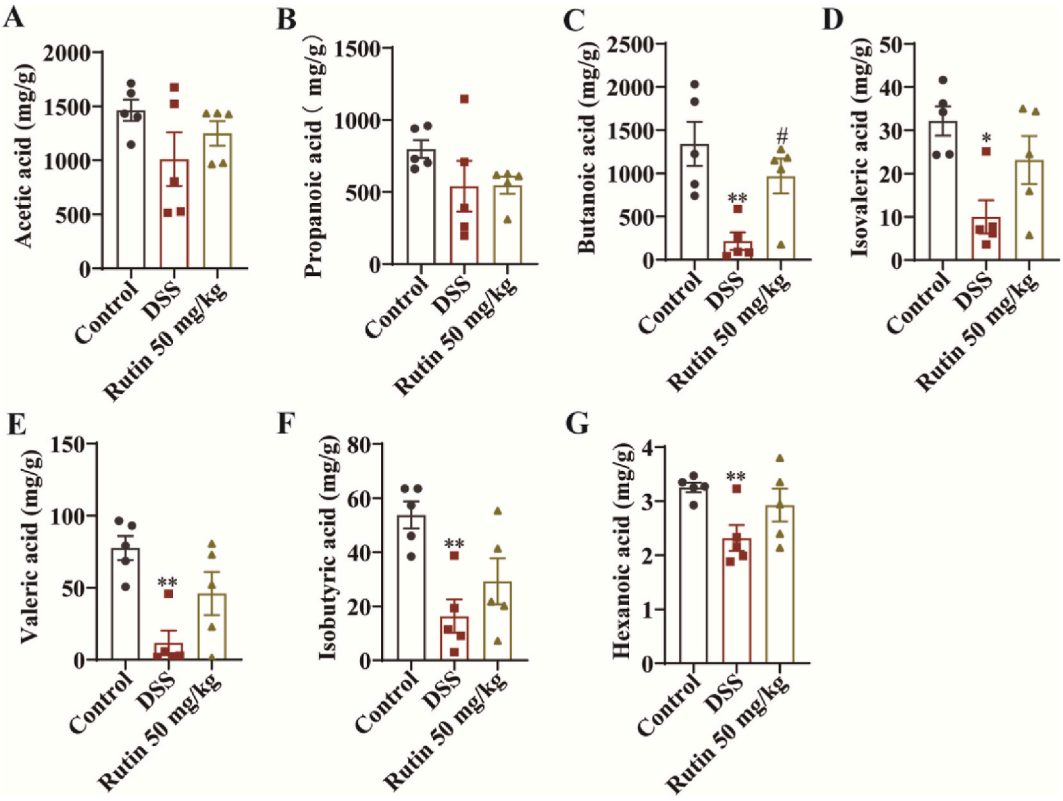

Fig. 6. Effect of rutin on SCFA production in mice with DSS-induced colitis. **(A)** Acetic acid; **(B)** Propionic acid; **(C)** Butyric acid; **(D)** Isobutyric acid; **(E)** Valeric acid; **(F)** Isovaleric acid; **(G)** Hexanoic acid. Data are expressed as the means ± SEMs ($^{*}P < 0.05$, $^{**}P < 0.01$, $^{***}P < 0.001$ vs Control group; $^{\#}P < 0.05$, $^{\#\#}P < 0.01$, $^{\#\#\#}P < 0.001$ vs DSS group), n = 6.

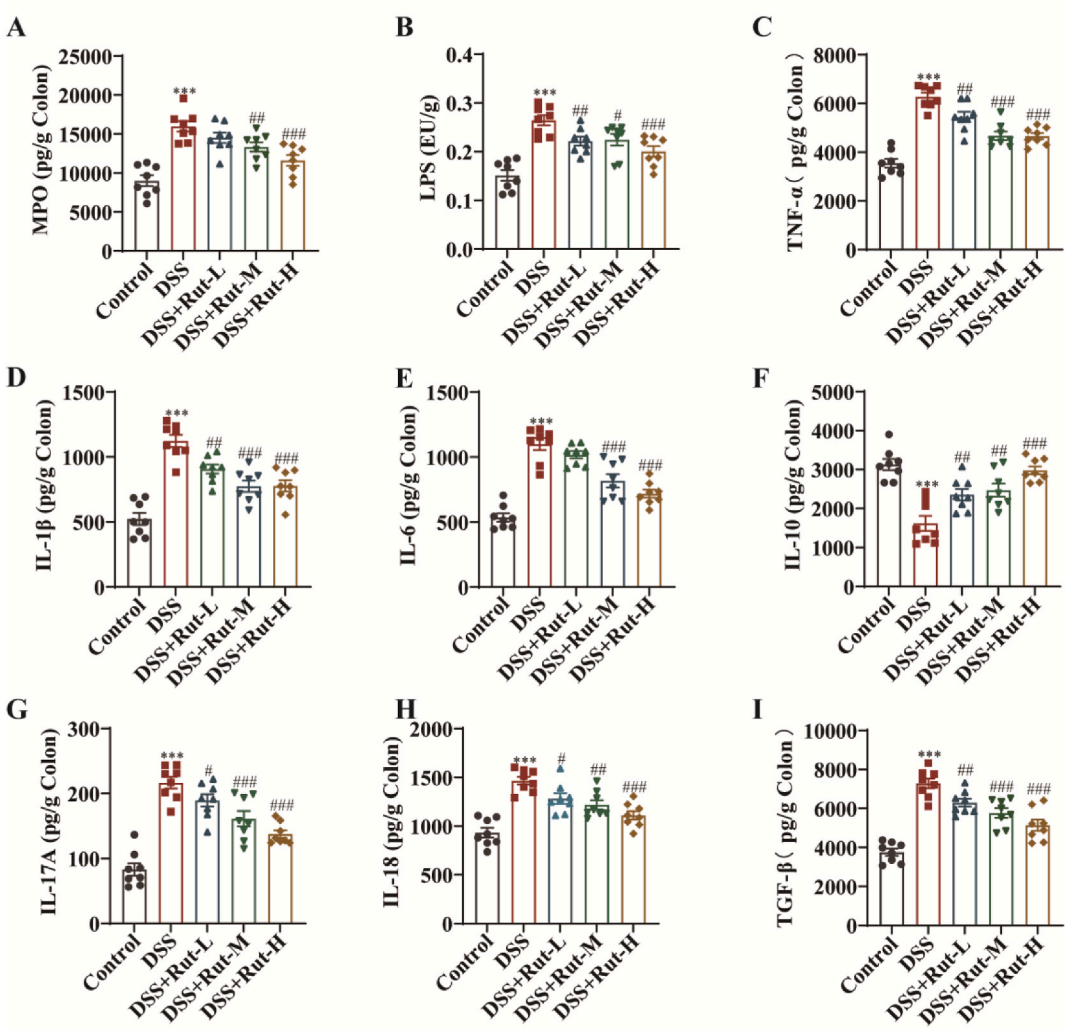

Fig. 7. Rutin ameliorates inflammation in the colonic tissue of mice with DSS-induced colitis. **(A, B)** Kits were employed to assess MPO and LPS levels in colonic tissues; **(C–I)** ELISA was utilized to determine proinflammatory cytokine (TNF-α, IL-1β, IL-6, TGF-β, IL-17A, IL-18) and anti-inflammatory cytokine (IL-10) levels in colonic tissues. Data are expressed as the means ± SEMs ($^{*}P < 0.05$, $^{**}P < 0.01$, $^{***}P < 0.001$ vs Control group; $^{\#}P < 0.05$, $^{\#\#}P < 0.01$, $^{\#\#\#}P < 0.001$ vs DSS group), n = 8.

homeostasis.

2.6. *Rutin contributes to the maintenance of intestinal mucosal barrier function in mice with DSS-induced colitis*

Our study revealed that rutin significantly augmented the abundance of the beneficial intestinal bacterium *Muribaculaceae*, which has been positively associated with the barrier functionality of the intestinal mucus layer and complex carbohydrate degradation [[26]]. Colonic goblet cells, key producers and secretors of mucus, play a pivotal role in preserving the mucosal barrier of the colon and thwarting microorganism invasion into the lumen. A characteristic feature of both DSS-induced colitis and ulcerative colitis (UC) in patients is goblet cell loss [[22]]. Therefore, Alcian Blue/Periodic Acid-Schiff (AB/PAS) staining was utilized to detect goblet cells within the colonic tissue. The results indicated that DSS treatment led to a marked loss of epithelial goblet cells in murine colonic tissue and a decrease in mucosal layer thickness, whereas rutin treatment increased goblet cell counts and considerably preserved colonic mucosa (Fig. 8A). Critical to the maintenance of intestinal mucus barrier function is the formation and distribution of interepithelial protein complexes between epithelial cells, encompassing TJs and AJs. The expression and distribution of TJ complexes (ZO-1, Occludin) and AJ proteins (E-cadherin, β-catenin, VE-cadherin) within the colon were assessed via immunofluorescence staining and Western blot experiments. Immunofluorescence staining revealed that DSS treatment resulted in a significant decrease in ZO-1, Occludin, and E-cadherin in colonic tissue, with their structures appearing discontinuous in the inner layer of the colonic epithelium. Rutin, however, substantially elevated the expression of these interepithelial complexes within the intestinal mucosal layer (Fig. 8B). Western blot analyses further established that DSS treatment significantly reduced the expression of ZO-1, Occludin,

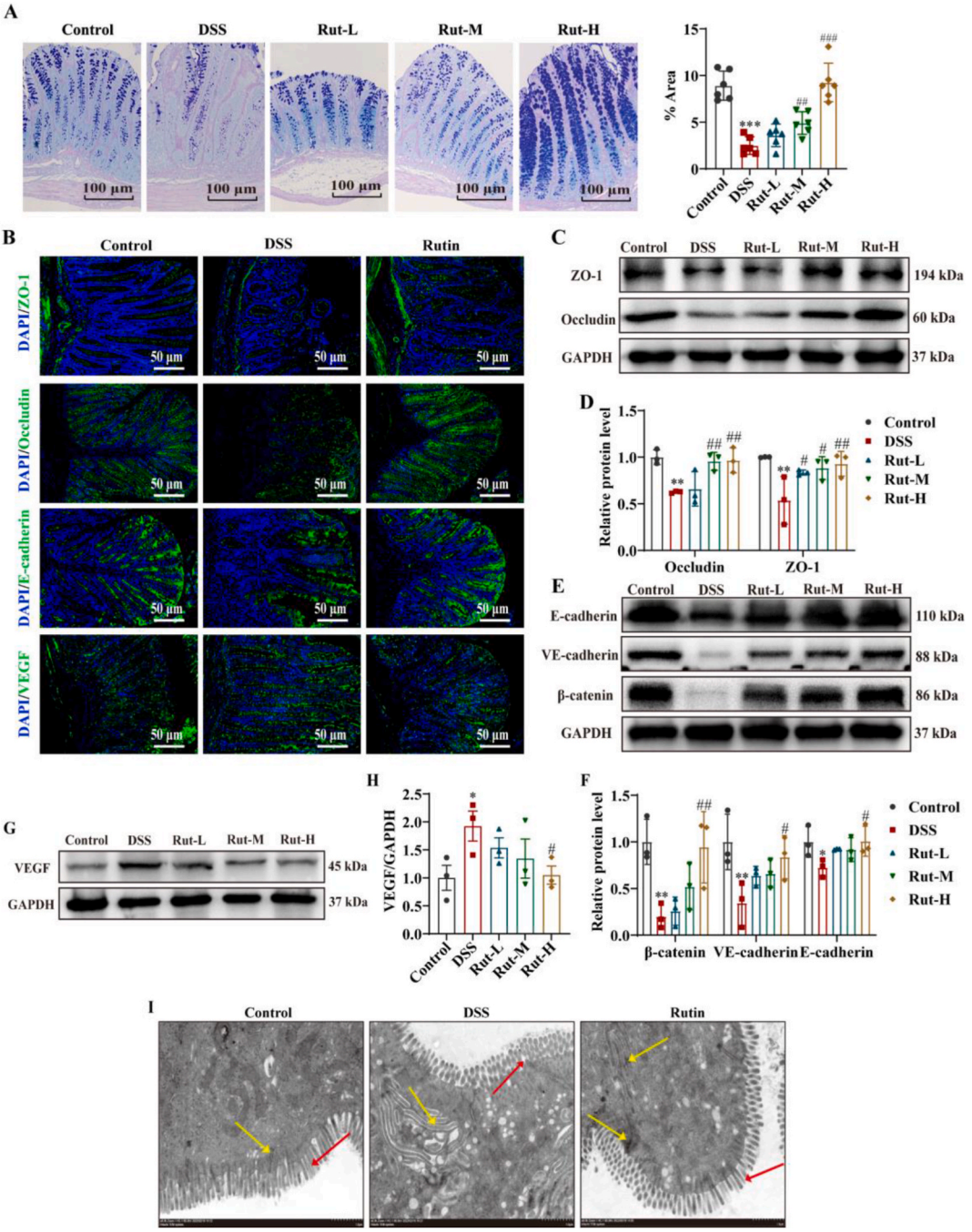

Fig. 8. Rutin enhances colonic epithelial integrity and TJ and AJ protein expression in DSS-induced colitis mice. **(A)** Representative AB-PAS staining images and analysis of goblet cell numbers in colonic tissues of each group (scale bar, 100 μm), n = 8; **(B)** Representative immunofluorescence images depicting in situ expression of TJ proteins (ZO-1, Occludin), AJ proteins (E-cadherin), and VEGF proteins (scale bar, 50 μm). **(C–H)** Representative immunoblots and relative expression levels of AJ proteins, TJ proteins, and VEGF proteins; **(I)** TEM displays representative images of colonic epithelial microstructure (scale bar, 1 μm), Red arrow: villi layer; yellow arrow: tightly connected structure. Data are expressed as the means ± SEMs ($^{*}P < 0.05$, $^{**}P < 0.01$, $^{***}P < 0.001$ vs Control group; $^{\#}P < 0.05$, $^{\#\#}P < 0.01$, $^{\#\#\#}P < 0.001$ vs DSS group), n = 8.

E-cadherin, β-catenin, and VE-cadherin proteins within colonic tissues, whereas rutin treatment reversed this effect in a dose-dependent manner (Fig. 8C–F). Additionally, our observations showed that DSS treatment elevated the expression levels of the VEGF protein in colon tissue, a trend that rutin treatment effectively counteracted (Fig. 8G and H). Consistent with these findings, rutin greatly mitigated the damage to the fine structure of the colonic mucosal epithelial tissue caused by DSS (Fig. 8I). Collectively, these results propose that rutin can improve DSS-induced damage to intestinal epithelial integrity by preserving goblet cell functionality and

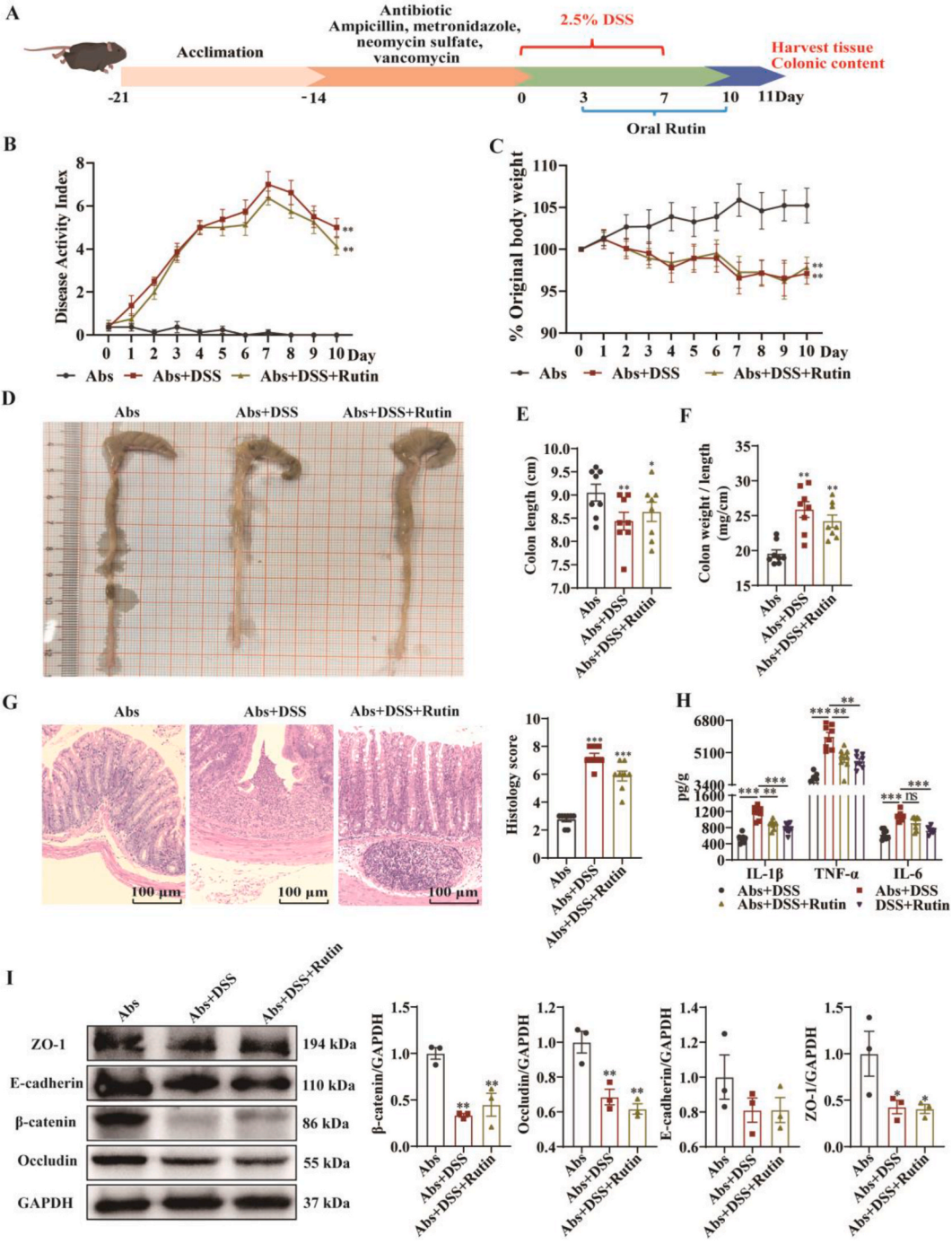

Fig. 9. Effect of rutin on mice with pseudosterile colitis. **(A)** Experimental design of rutin's effect on antibiotic-mediated intestinal flora depletion in colitis mice; **(B)** body weight change; **(C)** DAI score; **(D)** representative images of colons in each group of mice; **(E)** colon length; **(F)** colon weight/length ratio; **(G)** representative images of HE-stained colon tissue (scale bar, 100 μm) and histopathological scores in each group; **(H)** expression levels of TNF-α, IL-1β, and IL-6 in colonic tissue; **(I)** WB detection of tight junction and adhesion junction protein levels in colonic tissue. Data are expressed as the means ± SEMs (*$P < 0.05$, **$P < 0.01$, ***$P < 0.001$ vs Control group; $^{\#}P < 0.05$, $^{\#\#}P < 0.01$, $^{\#\#\#}P < 0.001$ vs DSS group), n ≥ 6.

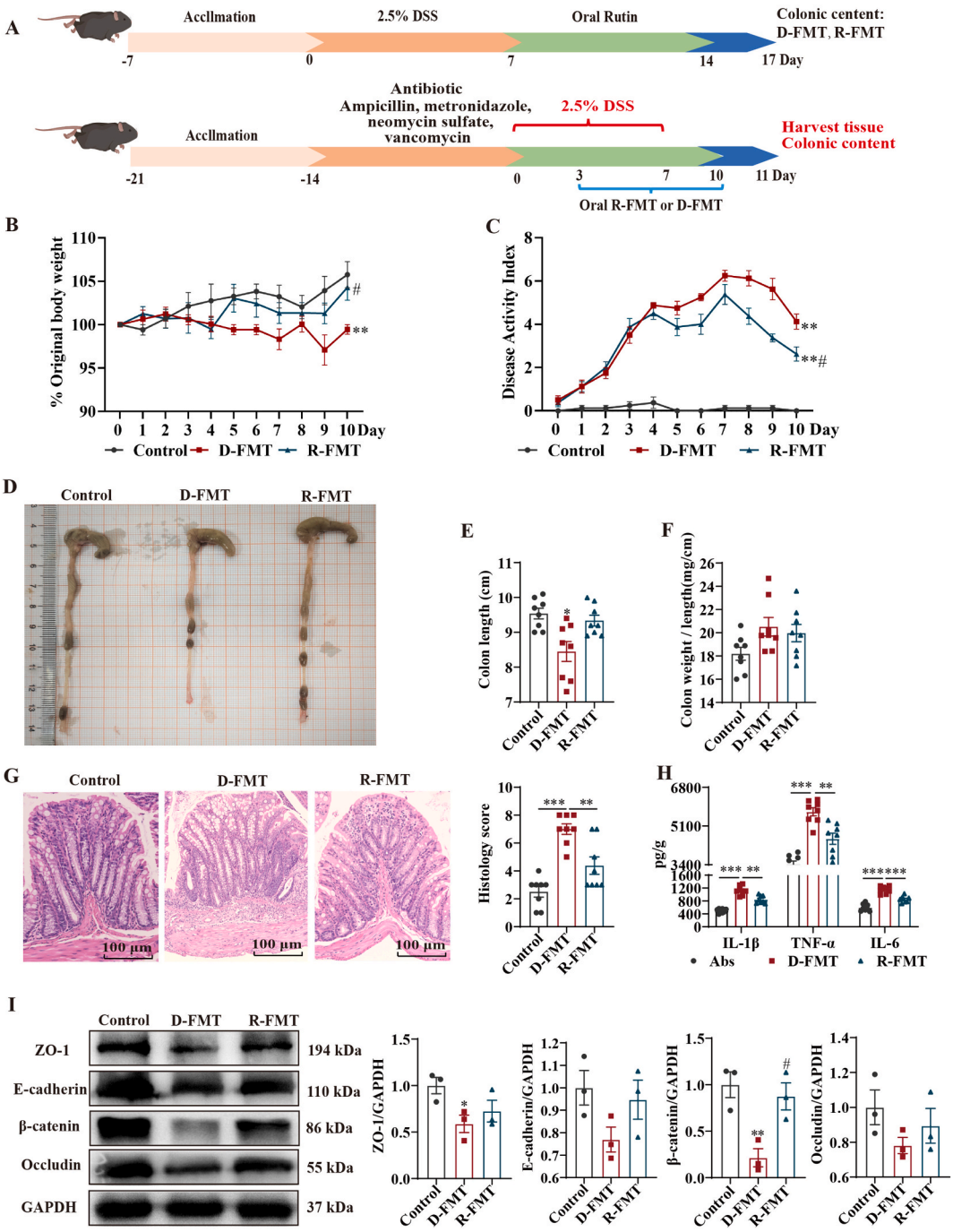

Fig. 10. Effect of rutin-treated mouse fecal transplants on mice with pseudogerm-free colitis. **(A)** Experimental design illustrating the impact of fecal transplantation from rutin-administered mice on antibiotic-mediated depletion of intestinal flora in colitis mice; **(B)** body weight change; **(C)** DAI score; **(D)** representative images of colons in each group of mice; **(E)** colon length; **(F)** colon weight/length ratio; **(G)** representative images of HE-stained colon tissue (scale bar, 100 μm) and histopathological scores in each group; **(H)** expression levels of TNF-α, IL-1β, and IL-6 in colonic tissue; **(I)** WB detection of tight junction and adhesion junction protein levels in colonic tissue. Data are expressed as the means ± SEMs ($^{*}P < 0.05$, $^{**}P < 0.01$, $^{***}P < 0.001$ vs Control group; $^{\#}P < 0.05$, $^{\#\#}P < 0.01$, $^{\#\#\#}P < 0.001$ vs DSS group), n ≥ 6.

boosting the expression of TJ and AJ proteins associated with intestinal epithelial tissue.

2.7. Rutin improves intestinal mucosal integrity and intestinal inflammation in mice with DSS-induced colitis by targeting the intestinal microbiota

To explore the role of gut microbiota in rutin's protective effect on colitis in mice, a pseudosterile mouse model was instituted via the administration of broad-spectrum antibiotics to healthy mice, which effectively depleted the majority of the gut microbiota (Fig. 9A). In order to verify whether Abs treatment depletes the intestinal microbiota, we referred to the criteria established by Yang et al. [[27]]. We collected the contents of the colonic tissues of mice in different treatment groups to remove the particulate matter by centrifugation, and the supernatants were taken for in vitro culturing of intestinal microorganisms. The results showed that no growing bacteria were found in the culture system in the negative blank control group (medium only) as well as in the Abs-treated groups (Abs, Abs + DSS and Abs + DSS + Rutin), except for the normal mouse group (Supplementary Fig. S2). It is suggested that the antibiotic mixture treatment depleted a large portion of the gut microbiota of the mice. Notably, in microbiota-depleted, antibiotic-treated colitis mice, rutin could not efficiently counterbalance the weight loss and the increased Disease Activity Index (DAI) scores incited by DSS treatment (Fig. 9B and C), and it only marginally lengthened the colon and reduced the colon weight-to-length ratio (Fig. 9D–F). Histopathological scrutiny suggested that rutin did not significantly mitigate colonic tissue crypt deformation in pseudosterile colitis mice and could not significantly reduce the elevated histopathological scores resulting from inflammatory cell infiltration (Fig. 9G–H). Moreover, in pseudosterile colitis mice, the modulating effect of rutin on the levels of IL-1β and IL-6 in colonic tissue was less pronounced, with no notable protection observed for TNF-α (Fig. 9I). Further immunoblotting experiments revealed that the modulatory effects of rutin on TJ proteins (ZO-1 and Occludin) and AJ proteins (E-cadherin, β-catenin, and VE-cadherin) were inhibited (Fig. 9J–K). These findings suggest that rutin's enhancement of intestinal mucosal barrier function and its ameliorating effects on DSS-induced colitis symptoms are dependent on the presence of intestinal flora.

To further corroborate the causal role of the gut microbiota in the rutin treatment of colitis, feces from both untreated and rutin-treated colitis mice were transplanted into pseudosterile colitis mice (Fig. 10A). The results demonstrated that rutin-treated fecal microbiota transplantation (R-FMT) in colitis mice mitigated general colitis symptoms such as weight loss, increased DAI scores, shortened colon length, and heightened histopathology scores in pseudosterile colitis mice compared to fecal transplants from untreated colitis mice, which did not exhibit significant therapeutic effects (Fig. 10B–G). Examination of colonic cytokines also revealed that fecal transplants from rutin-treated mice significantly reduced the levels of IL-1β, IL-6, and TNF-α (Fig. 10H). Western blotting experiments showed that fecal transplants from rutin-treated colitis mice increased the expression of tight junction proteins (ZO-1, Occludin) and adhesion junction proteins (E-cadherin, β-catenin), thereby promoting the restoration of the intestinal epithelial barrier in pseudosterile colitis mice (Fig. 10I). Conclusively, the results validate the beneficial effect of rutin on the loss of intestinal mucosal integrity and intestinal inflammation induced by DSS administration, an effect that can be attributed to the presence of intestinal flora.

3. Discussion

Polyphenolic compounds are widely recognized for their ability to improve intestinal health by influencing barrier function, gut microbiota composition, signaling pathways, and immune responses [[14]]. Distiller's grains, a byproduct of winemaking derived from grains such as sorghum and fruits such as grapes, serve as a natural reservoir of phenolic compounds that boasting potent antioxidant and biological traits. Globally, the abundance of this byproduct makes it an excellent source of phenolic compounds relevant for the nutraceutical, pharmaceutical, and cosmetic industries [[15]]. Despite this, the therapeutic effects and mechanisms of distiller's grain polyphenol extracts on colitis remain largely underinvestigated. This study deployed the LC-HR-ESI-MS/MS technique to dissect the composition of Moutai distiller's grain polyphenol extract. The analysis suggested that the extract was chiefly composed of rutin, quercetin, naringenin, and dihydroquercetin, with rutin being predominant. The study initially demonstrated that the Moutai distiller's grain polyphenol extract significantly ameliorated DSS-induced colitis in mice, as shown by improvements in key colitis markers such as DAI scores, weight loss, histopathological alterations, and inflammatory infiltration. Subsequently, due to the high enrichment of rutin in distiller's grain polyphenol extracts, its safety in vivo (even at elevated doses up to 5000 mg/kg), pharmacokinetic properties, and established efficacy in managing acute and chronic colitis, rutin was selected for further mechanistic exploration.

Extracellular mucus along with the epithelial junction complex, comprising of TJs and AJs, serve as pivotal components of the mucosal barrier that ward off harmful substances in the intestinal lumen, playing a crucial role in intestinal health [[28–30]]. Prior research has established that inflammatory factors such as IL-6, IL-1β, and TNF-α trigger the downregulation of TJ proteins, thereby increasingintestinal paracellular permeability, allowing the infiltration of proinflammatory factors from the intestinal lumen into the mucosal tissue and activating the mucosal immune system, which leads to sustained inflammation and tissue damage [[31,32]]. Rutin has been demonstrated to fortify the mucus layer and epithelial barrier permeability by modulating the mRNA levels of MUC2, ZO-1, and Occludin [[18]]. In this study, rutin not only increased goblet cell counts and elevated the expression of TJ proteins (ZO-1 and Occludin), but also diminished the levels of the cytokine IL-18 and inflammatory factors (IL-1β, IL-6, and TNF-α), impacting goblet cell maturation in colonic tissue, further underscoring the protective influence of rutin on the intestinal mucus layer and the intestinal epithelial barrier. Additionally, AJ serves as the primary intercellular adhesion structure among epithelial cells, with classical cadherins being its fundamental component. E-cadherin is localized in the epithelium of colonic crypts, and loss of E-cadherin not only affects the density and structure of the epithelium but also impacts the maturation and localization of goblet and Paneth cells, thereby impairing mucus production and augmenting susceptibility to bacterial infection [[33]]. In this investigation, rutin supplementation

not only ameliorated epithelial tight junctions but also boosted the expression of adhesion-related proteins (E-cadherin, VE-cadherin, and β-catenin), bolstering epithelial adherens junctions and restoring intestinal epithelial barrier integrity. Furthermore, increased VEGF levels and MPO activity were noted in the colonic tissues of DSS-treated mice. Elevated VEGF expression has been linked directly to pathological angiogenesis and inflammation in both human and experimental colitis [[34]]. Rutin markedly downregulated VEGF expression levels and MPO activity, suggesting its potential role in protecting vascular endothelial barrier function. In essence, these findings substantiate the potential role of rutin in preserving intestinal barrier function, largely through the modulation of goblet cells and the expression of TJ and AJ proteins. The influence of rutin extends to controlling key inflammatory cytokines and factors, reinforcing the importance of this polyphenolic compound in mitigating the effects of colitis. Furthermore, rutin's capacity to reduce the expression of VEGF, a key player in pathological angiogenesis, underscores its therapeutic potential in maintaining the integrity of vascular endothelial barriers. Therefore, these findings accentuate the potential of rutin as a candidate for therapeutic intervention in colitis, paving the way for further investigations into the applications of polyphenolic compounds in the treatment of inflammatory conditions.

Gut microbiota dysregulation may precipitate intestinal epithelial cell dysfunction and mucosal damage, instigating intestinal inflammation. Moreover, alterations in the gut microbiota alterations may potentiate colitis-related tumorigenesis through the perpetuation of chronic inflammation and the production of carcinogens [[35]]. Existing literature suggests that rutin can palliate DSS-induced colonic inflammation in mice by impeding the production and activation of inflammatory mediators, modulating immune cell activity and cytokine secretion, and bolstering the intestinal mucosal barrier to mitigate intestinal inflammation. This, however, seems paradoxical given rutin's low bioavailability [[19]]. Recent insights recognize rutin's capacity to interact with intestinal microbiota. For instance, Yan et al. underscored the ability of rutin supplementation to intervene in obesity and hyperlipidemia development in mice induced by a high-fat diet by targeting intestinal flora and ameliorating obesity-related metabolic disorders [[36]]. In vitro studies have shown rutin's potent antimicrobial activity against a variety of pathogens, suggesting that rutin may serve as a prebiotic in the intestinal tract, which could partially account for its in vivo action. In this investigation, an analysis of the gut flora structural analysis at the phylum level unveiled a significant increase in the abundance of *Campilobacterota* and *Proteobacteria* abundance in the DSS-treated group, aligning with previous findings. *Campilobacterota's* unique and diverse pathogenic potential positions it as a likely contributor to IBD pathogenesis [[37]]. *Proteobacteria* transformation is frequently associated with intestinal flora disorders and IBD pathogenesis [[13,38]]. Rutin therapy counteracted the dysbiosis induced by DSS, enhancing Firmicutes abundance and moderately reducing *Verrucomicrobiota* and *Deferribacterota* abundance. At the family level, *Bacteroidaceae*, *Enterobacteriaceae*, *Erysipelatoclostridiaceae*, *Helicobacteraceae*, and *Veillonellaceae* were markers of the DSS group, with their abundance significantly reduced following rutin treatment, alongside a significant increase in the Muribaculaceae group. Variance analysis (genus level) and LEfSe (LDA>4) revealed a markedly higher abundance of *Bacteroides*, *Helicobacter*, *Klebsiella*, and *Veillonella* in the DSS group, with their abundance significantly reduced in the rutin group, and an increased abundance of *Ruminococcus_torques_group*, *Lachnoclostridium*, and *norank_f_Muribaculaceae*. These findings suggest that rutin therapy may foster positive functional regulation of specific bacteria, curtail the growth conditions of pathogenic bacteria, and assist in reestablishing intestinal barrier function. Importantly, the depletion of gut microbiota via antibiotic treatment curtailed rutin's efficacy in alleviating colitis symptoms, highlighting the gut microbiota's role in rutin's colitis relief function. This study further demonstrated that rutin supplementation-mediated FMT significantly mitigated the colitis signs and pathological changes induced by DSS, effectively alleviating colitis symptoms in recipient mice, underlining the critical role of intestinal microbiota remodeling in the biological activity of rutin.

LPS and SCFAs, classical indicators of the intestinal system and microbiota function, are two metabolites originating from the intestinal flora [[39]]. The intestinal lumen harbors LPS, produced by gram-negative bacteria, and in situations of intestinal microbial imbalance, a surge in detrimental bacteria results in excessive LPS release. When the integrity of the intestinal mucosa is compromised, it becomes porous, facilitating LPS invasion into the mucosa and bloodstream, which can trigger systemic and targeted inflammation via TLR4 signaling pathway activation [[40]]. This study found that rutin significantly curtailed the abundance of certain LPS-producing bacteria, such as *Helicobacter*, *Klebsiella*, and *Veillonella*, which are implicated in colitis development. This led to a decrease in LPS levels within the colonic tissue, thereby assuaging intestinal inflammation. Moreover, SCFAs derived from gut microbiota play a pivotal role in maintaining intestinal immune homeostasis through their anti-inflammatory and immunosuppressive properties [[41]]. Predominant SCFAs in the intestine include acetic, propionic, and butyric acid, while isobutyric, valeric, and isovaleric acids are found in smaller amounts. Previous reports suggest that SCFAs can modulate colonic Treg differentiation and function, thwarting DSS-induced colitis. The dynamic balance between Treg and Th17 cells is crucial for intestinal microecosystem homeostasis, a process that can be regulated by microbiota-derived SCFA signaling [[42]]. Treg cells are characterized by the expression of the specific transcription factor Foxp3. They inhibit other immune cells, notably Th17 cells, and secrete the anti-inflammatory cytokine IL-10, thereby mitigating the immune response and inflammation. Prior research has shown that rutin modulates NF-κB signaling and the Treg axis, ameliorating symptoms of DSS-induced colitis [[19]]. This study revealed that rutin supplementation enhanced the production of SCFAs, particularly butyric acid, from the microbial community. Remarkably, all genera that increased in the rutin-treated group were associated with SCFA production. Earlier research reported that *Ruminococcus_torques_group* enhances SCFA levels and mitigates colitis symptoms in DSS-treated mice [[43]]. *Lachnoclostridium*, a butyric acid producer, effectively stabilizes intestinal homeostasis through its anti-inflammatory and immunosuppressive properties [[44]]. *norank_f_Muribaculaceae* is known to boost SCFA production and ameliorate intestinal mucosal inflammation [[45,46]]. Butyric acid, a primary energy source for colon cells, has been shown to elicit an anti-inflammatory response by inhibiting the NF-κB pathway, downregulating proinflammatory gene expression, regulating Treg cells, and elevating IL-10 levels [[43,47]]. Additionally, this study indicated that rutin treatment led to a significant upregulation of IL-10 expression and downregulation of proinflammatory cytokines

like IL-17A and IL-6, thereby reducing intestinal inflammation. This implies that the beneficial effects of rutin on intestinal inflammation may be tied to the regulation of intestinal microbial homeostasis, promotion of SCFA production, and modulation of downstream signaling.

4. Conclusions

In conclusion, this study pioneers the demonstration that MDGP can alleviate DSS-induced colitis symptoms in mice and comprehensively analyzes its chemical composition. Furthermore, rutin, its principal active ingredient, was employed as a therapeutic target to unravel the anti-colitis mechanism. The findings suggest that rutin's anti-inflammatory mechanism may encompass the downregulation of harmful bacteria such as *Helicobacter*, *Klebsiella*, and *Veillonella*, an increase in beneficial bacteria such as *Ruminococcus_torques_group*, *Lachnoclostrium*, and *norank _f_ Muribaculaceae*, reduction in intestinal LPS levels, stimulation of butyric acid production, enhancement of tight junction and adherens junction structures, amelioration of intestinal mucosal barrier integrity, and mitigation of inflammatory infiltration. Importantly, this study verified through fecal microbiota transplantation (FMT) and antibiotic depletion experiments that the intestinal microbiota is a critical component of the effect of rutin on mucosal barrier function and inflammation regulation. Significantly, this study suggests that rutin and polyphenol-rich MDGP serve as potential dietary resources for colitis treatment, offering novel insights into the utilization of distiller grain polyphenol extracts as nutraceuticals and the repurposing of distiller grain resources. This paves the way for future exploration of the potential therapeutic effects of dietary components in colitis management, shedding light on the complex interactions between diet, gut microbiota, and host health.

5. Materials and methods

5.1. Materials

Moutai distiller grains were generously supplied by Kweichow Moutai Co., Ltd. Various chemical reagents, including sodium dextran sulfate (36–50 kDa), mesalazine, rutin, neomycin sulfate, ampicillin, metronidazole, and vancomycin, were procured from Shanghai Maclean Biochemical Co. (Shanghai, China). Occult blood test kits were sourced from Beijing Reagan Biotechnology Co (Beijing, China). Kits to assay MPO, LPS, and ELISA for TNF-α, TGF-β, IL-1β, IL-6, IL-10, IL-17A, and IL-18 were obtained from Shanghai Enzyme Link Biotechnology Co. (Beijing, China). Rabbit antibodies against occludin, ZO-1, and E-cadherin were purchased from CST (Danvers, USA), while rabbit anti-VE-cadherin and anti-β-catenin antibodies were purchased from Abcam (CA, USA). Rabbit anti-VEGF and mouse anti-GAPDH antibodies were acquired from Proteintech (Wuhan, China).

5.2. Evaluation of Moutai Distiller's grains Polyphenol Extract's effects on DSS-induced colitis

5.2.1. Extraction and purification of polyphenolic compounds from Moutai distiller grains

The polyphenol extraction process was adapted from the methodology devised by Ashley et al., with minor alterations [[48]]. Moutai distiller grains were amalgamated with 70 % ethanol in a 1:25 (m/v) ratio, and this blend was subjected to a 2-h reflux extraction. This extraction operation was repeated once, and the extracts were then combined and sieved through a 200-mesh filter. The resulting filtrate underwent concentration to eliminate ethanol, producing crude polyphenols. Further purification was achieved using D101 macroporous adsorption resin, culminating in the creation of Moutai distiller's grain polyphenol extract (MDGP).

5.2.2. Establishment of the DSS-induced colitis model and evaluation of Pharmacological efficacy

Male C57BL/6J mice (7–8 weeks old, 20 ± 2 g) were procured from Changzhou Cavins Laboratory Animal Co., Ltd. (Changzhou, Jiangsu, China) [SCXK (su) 2021-0013] and provided unrestricted access to food and water. Mice were maintained under controlled conditions (temperature: 25 ± 2 °C; humidity: 65 %; light/dark cycle: 12 h). The animal study was approved by the Ethics Committee of China Pharmaceutical University.

Following a 7-day acclimation period, all mice, except those in the normal control group, received 2.5 % DSS (w/v, distilled water) solution in place of their drinking water to establish a colitis model [[49]]. Grouping was carried out according to the criteria outlined by Ni et al. [[50]]., which included the model group (DSS), the mesalazine group (5-ASA, 200 mg/kg), and the distiller's grain polyphenol extract groups (50, 100 mg/kg). Treatments were administered once daily for a consecutive 7-day period. Mice were monitored daily for alterations in body weight, fecal characteristics, and occult blood presence. At 24 h postfinal treatment, mice were euthanized, their colons were excised and cleansed with prechilled PBS, and both colon length and weight were documented. A 0.5 cm distal colon segment was obtained for histopathological examination.

5.2.3. Component analysis of polyphenolic compounds

Moutai Distiller's Grains Polyphenol Extract (MDGP) samples were subjected to LC-HR-ESI-MS/MS analysis. Chromatographic separation occurred on an Agilent 1260 Phenomenex Luna C18 analytical column (250 × 4.6 mm, 5 μm) with a mobile phase comprising acetonitrile (A) and water (B) containing 0.1 % (v/v) formic acid. The gradient elution conditions were as follows: 0–20 min, 20–100 % A; 20–30 min, 100 % A. The MDGP injection volume was set at 10 μL, with four reference compounds (rutin, quercetin, dihydroquercetin, and naringenin) injected at 5 μL, at a column temperature of 25 °C and a flow rate of 1 mL/min. Detection using Bruker maXis Q-TOF in positive ion-mode. The MS parameters of the positive ion modes were as follows: dry temperature,180 °C; dry gas, 4 L/min; reference masses were recorded at an m/z range of 200–700.

5.3. Investigation of Rutin's mechanism of action against DSS-induced colitis

The establishment of a DSS-induced colitis model was carried out as previously detailed. Randomization of groups was conducted based on DAI scores, which included the model group (DSS), the mesalazine group (5-ASA, 200 mg/kg), and the rutin group (12.5 mg/kg, 25 mg/kg, 50 mg/kg). The specified drug was dispensed daily for a seven-day period. Mice were euthanized 24 h post-final dosage, and the complete colon was excised. Colon contents were transferred under sterile conditions into sterilized EP tubes, instantly frozen in liquid nitrogen, and kept at −80 °C for subsequent analysis. The colon was rinsed with prechilled PBS, and the dimensions were recorded. A distal colon segment of 0.5 cm was reserved for histopathological analysis and immunofluorescence staining, whereas the remaining colon tissue was snap-frozen in liquid nitrogen for molecular biology assays.

5.4. Fecal Microbial Transplantation

A pseudogerm-free (PGF) mouse model was developed by giving the mice free access to a water solution containing a cocktail of antibiotics (vancomycin 0.2 g/L, ampicillin 0.5 g/L, metronidazole 0.5 g/L, and neomycin sulfate 0.5 g/L) for 14 days before DSS induction. The aim was to deplete the intestinal commensal microbiota substantially [[51]]. Fecal microbiota transplantation (FMT) was performed with slight alterations from the procedure described earlier [[52]]. Colitis was induced in donor mice that were then provided with either standard drinking water (control) or rutin (50 mg/kg). Recipient mice were given the antibiotic mixture solution for 14 days to ensure significant gut microbiota eradication, followed by a 7-day induction with 2.5 % DSS. Simultaneously, fresh feces from colitis-stricken (D-FMT) or rutin-treated (R-FMT) donor mice were transplanted daily. FMT initiation occurred three days postfinal rutin administration, with fecal sample transplantation carried out as usual. Fecal samples from random donor mice were diluted 1:10 (w/v) with saline, vortexed for 1 min to homogenize, and centrifuged at 500×*g* for 3 min to eliminate particulate matter. The supernatant was collected and orally dispensed to each recipient mouse within a 10-min window at a volume of 200 μL to avert bacterial component changes.

5.5. Histological evaluation and immunofluorescence analysis

To evaluate crypt deformation, structural damage, inflammatory cell infiltration, and ulceration, colon sections underwent staining with hematoxylin and eosin (HE) according to standard procedures. Paraffin-embedded colon sections were subjected to Alcian Blue-Periodic Acid Schiff (AB-PAS) staining to investigate mucus epithelium thickness and the presence of goblet cells. Immunofluorescence assays were deployed on colonic tissues to scrutinize epithelial barrier function, specifically focusing on the tight junction proteins Occludin and ZO-1 and the adherens junction protein E-cadherin.

5.6. Transmission electron Microscopy (TEM)

For further analysis, a 5 mm segment of fresh colon tissue was rinsed with prechilled PBS and promptly immersed in a 2.5 % glutaraldehyde fixative solution. Following a 2-h fixation period at room temperature, the tissue underwent an overnight incubation at 4 °C in fresh 2.5 % glutaraldehyde. Postincubation, the tissue was rinsed with PBS and then fixed for another 2 h at room temperature in 0.1 M PBS containing 1 % osmium tetroxide before dehydration. The dehydrated tissue was then embedded in Epon 812 with acetone for an overnight period. Subsequently, the tissue was embedded in pure Epon 812 and allowed to cure for 48 h at 60 °C in an oven. Ultrathin sections of 60–80 nm thickness were cut using an ultramicrotome and then placed onto 150-mesh square formvar copper grids. Staining was performed in the dark for 8 min with 2 % uranyl acetate in saturated alcohol, followed by an 8-min room temperature stain with 2.6 % lead citrate. A transmission electron microscope was employed to acquire images and observe the tight junction structures within the colonic tissue.

5.7. Inflammatory cytokine content of colonic tissue assay

The concentrations of MPO, TNF-α, LPS, IL-1β, IL-6, TGF-β, IL-17A, IL-18, and IL-10 in colon tissue were quantified via ELISA kits, adhering strictly to the guidelines provided by the manufacturers.

5.8. Western blotting

Colon tissue protein lysates were prepared from frozen samples using a protein lysis buffer replete with protease and phosphatase inhibitors. The concentration of the resultant protein was determined utilizing the BCA Protein Assay Kit. Protein aliquots (30–60 μg) were separated using SDS−PAGE gels and subsequently transferred onto polyvinylidene difluoride (PVDF) membranes. Nonspecific proteins were blocked using a 5 % (w/v) skim milk powder solution at room temperature for an hour. Membranes were then probed with primary antibodies (occludin, ZO-1, β-catenin, E-cadherin, VE-cadherin, and VEGF) during an overnight incubation at 4 °C. After incubation, the membranes were rinsed with TBST and then exposed to secondary antibodies for an hour at room temperature. Protein bands were visualized via chemiluminescent reagents and the Bio-Rad image analysis system, with protein quantification performed using Image Lab software.

5.9. Gut microbial gene sequencing

After extraction of the microbial community DNA from the mouse colon's luminal content, the quality of the DNA was assessed using a NanoDrop 2000 spectrophotometer and 1 % agarose gel electrophoresis. The bacterial 16S rRNA gene's V3–V4 hypervariable region was then amplified via polymerase chain reaction (PCR) using the primers 338F (5′-actcctacgggaggcagcag-3′) and 806R (5′-ggactachvgggtwtctaat-3′). The PCR products were recovered from the gel using an AxyPrepDNA Gel Recovery Kit (Axygen) and quantified utilizing the QuantiFluor™-ST Blue Fluorescence Quantification System (Promega). The sequencing volume requirements of each sample dictated the proportions for pooling. The library was constructed according to the TruSeqTM DNA Sample Prep Kit protocol, and pair-end (PE) sequencing was executed on the Illumina MiSeq platform by Shanghai Majorbio Biopharm Technology Co., Ltd. (Shanghai, China). Following library amplification, the raw data underwent quality control using FASTP v 0.19.6 software. FLASH v1.2.11 software was employed for assembly, while chimeric sequences were eliminated using the UCHIME method. Clustering of operational taxonomic units (OTUs) was performed using the USEARCH7-uparse clustering method in UPARSE v 7.0.1090 software with a similarity cutoff set at 97 %. Analyses of α-diversity, β-diversity, community composition, and LEfSe were conducted on the cloud-based platform available at https://cloud.majorbio.com/.

5.10. Short-chain fatty acid analysis

Short-chain fatty acids (SCFAs) in the cecal content were quantified utilizing an Agilent 8890B–5977 B GC/MSD system (Agilent, CA, USA). Briefly, 25 mg of fecal sample was weighed, homogenized in 500 μL of water (containing 0.5 % phosphoric acid), and centrifuged at 4 °C for 15 min at 13,000 g. The supernatant was extracted with 200 μL of n-butanol solvent (containing 10 μg/mL of internal standard 2-ethylbutyric acid). The supernatant or standard was transferred to an autosampling vial and injected into the GC–MS for detection by vortexing for 10 s, an ice bath for 10 min, and centrifugation at 4 °C and 13000×*g* for 5 min. The quantitative analysis of SCFAs was evaluated by comparing the peak area of the test sample with that of 2-ethylbutyric acid (internal standard).

5.11. Statistical analysis

The data were interpreted using SPSS 24.0, GraphPad Prism 9.0 (GraphPad software), ImageJ, and Image Lab, with results conveyed as the mean ± standard error (SEM). The chi-square test confirmed the normal distribution of the measured data. Comparisons between multiple groups were executed using one-way ANOVA and LSD tests, while Student's *t*-test was applied for comparisons between two independent groups. Significance was denoted as $^{*}P < 0.05$, $^{**}P < 0.01$, $^{***}P < 0.001$.

Funding

This research was made possible through the support of the National Natural Science Foundation of China under grant numbers 82274073 and 81872986. Additional backing came from the "Double First-Class" University Project, with project identifier CPU2022QZ28.

Data availability

Data will be made available on request.

CRediT authorship contribution statement

Jin-hu Chen: Data curation, Investigation, Writing – original draft. **Cai-li Zhao:** Data curation, Formal analysis, Methodology, Validation. **Yong-su Li:** Data curation, Formal analysis. **Yu-bo Yang:** Software. **Jian-guang Luo:** Conceptualization, Funding acquisition. **Chao Zhang:** Conceptualization, Funding acquisition, Resources, Writing – review & editing. **Li Wang:** Conceptualization, Project administration.

Declaration of competing interest

The authors declare the following financial interests/personal relationships which may be considered as potential competing interests:Chao Zhang reports was provided by China Pharmaceutical University. If there are other authors, they declare that they have no known competing financial interests or personal relationships that could have appeared to influence the work reported in this paper.

Acknowledgments

We thank Ping Zhou, Xiaonan Ma (State Key Laboratory of Natural Medicines Public Platform, China Pharmaceutical University, Nanjing, China), Sufen Li (Department of Pathology, The First People's Hospital of Taizhou, Taizhou, China), and Yihao Che (South China Sea Institute of Oceanography, Chinese Academy of Sciences, China) for their assistance in the use of the inverted fluorescence microscope (Nikon Ts2R), the digital section scanner, the histopathological evaluation, and the LC-HR-ESI-MS/MS.

Appendix A. Supplementary data

Supplementary data to this article can be found online at https://doi.org/10.1016/j.heliyon.2023.e22186.

References

[1] A. Ahmad, K. Vaghasiya, A. Kumar, P. Alam, S.S. Raza, R.K. Verma, R. Khan, Enema based therapy using liposomal formulation of low molecular weight heparin for treatment of active ulcerative colitis: new adjunct therapeutic opportunity, Mater. Sci. Eng., C 121 (2021), 111851.
[2] Ulcerative colitis, Nat. Rev. Dis. Prim. 6 (1) (2020) 73.
[3] I. Ordas, L. Eckmann, M. Talamini, D.C. Baumgart, W.J. Sandborn, Ulcerative colitis, Lancet 380 (9853) (2012) 1606–1619.
[4] C.J. Hong, S.Y. Chen, Y.H. Hsu, G.C. Yen, Protective effect of fermented okara on the regulation of inflammation, the gut microbiota, and SCFAs production in rats with TNBS-induced colitis, Food Res. Int. 157 (2022), 111390.
[5] P.E. Dube, C.Y. Liu, N. Girish, M.K. Washington, D.B. Polk, Pharmacological activation of epidermal growth factor receptor signaling inhibits colitis-associated cancer in mice, Sci. Rep. 8 (1) (2018) 9119.
[6] M.L.Y. Wan, K.H. Ling, H. El-Nezami, M.F. Wang, Influence of functional food components on gut health, Crit. Rev. Food Sci. Nutr. 59 (12) (2019) 1927–1936.
[7] F. Xu, Y. Cheng, G. Ruan, L. Fan, Y. Tian, Z. Xiao, D. Chen, Y. Wei, New pathway ameliorating ulcerative colitis: focus on Roseburia intestinalis and the gut-brain axis, Therapeutic Advances in Gastroenterology 14 (2021), 17562848211004469.
[8] Y. Huang, Q. Yang, X. Mi, L. Qiu, X. Tao, Z. Zhang, J. Xia, Q. Wu, H. Wei, Ripened Pu-erh tea extract promotes gut microbiota resilience against dextran sulfate sodium induced colitis, J. Agric. Food Chem. 69 (7) (2021) 2190–2203.
[9] K. Wang, X. Jin, Y. Chen, Z. Song, X. Jiang, F. Hu, M.A. Conlon, D.L. Topping, Polyphenol-rich propolis extracts strengthen intestinal barrier function by activating AMPK and ERK signaling, Nutrients 8 (5) (2016).
[10] L. Cui, X. Guan, W. Ding, Y. Luo, W. Wang, W. Bu, J. Song, X. Tan, E. Sun, Q. Ning, G. Liu, X. Jia, L. Feng, Scutellaria baicalensis Georgi polysaccharide ameliorates DSS-induced ulcerative colitis by improving intestinal barrier function and modulating gut microbiota, Int. J. Biol. Macromol. 166 (2021) 1035–1045.
[11] C. Ye, L. Liu, X. Ma, H. Tong, J. Gao, Y. Tai, L. Huang, C. Tang, R. Wang, Obesity aggravates acute pancreatitis via damaging intestinal mucosal barrier and changing microbiota composition in rats, Sci. Rep. 9 (1) (2019) 69.
[12] D. Bai, T. Sun, J. Zhao, J. Du, X. Bu, W. Cao, Y. Zhao, N. Lu, Oroxylin A maintains the colonic mucus barrier to reduce disease susceptibility by reconstituting a dietary fiber-deprived gut microbiota, Cancer Lett. 515 (2021) 73–85.
[13] S. Li, Y. Chen, Y. Zhang, H. Lv, L. Luo, S. Wang, X. Guan, Polyphenolic extracts of coffee cherry husks alleviated colitis-induced neural inflammation via NF-kappaB signaling regulation and gut microbiota modification, J. Agric. Food Chem. 70 (21) (2022) 6467–6477.
[14] M.L.Y. Wan, V.A. Co, H. El-Nezami, Dietary polyphenol impact on gut health and microbiota, Crit. Rev. Food Sci. Nutr. 61 (4) (2021) 690–711.
[15] M.J. Jara-Palacios, Wine lees as a source of antioxidant compounds, Antioxidants-Basel. 8 (2) (2019) 45.
[16] P. Tapia-Quiros, M.F. Montenegro-Landivar, M. Reig, X. Vecino, J.L. Cortina, J. Saurina, M. Granados, Recovery of polyphenols from agri-food by-products: the olive oil and winery industries cases, Foods 11 (3) (2022).
[17] W.F. Hodnick, F.S. Kung, W.J. Roettger, C.W. Bohmont, R.S. Pardini, Inhibition of mitochondrial respiration and production of toxic oxygen radicals by flavonoids. A structure-activity study, Biochem. Pharmacol. 35 (14) (1986) 2345–2357.
[18] S. Sharma, A. Ali, J. Ali, J.K. Sahni, S. Baboota, Rutin : therapeutic potential and recent advances in drug delivery, Expet Opin. Invest. Drugs 22 (8) (2013) 1063–1079.
[19] A. Sharma, N.V. Tirpude, M. Kumari, Y. Padwad, Rutin prevents inflammation-associated colon damage via inhibiting the p38/MAPKAPK2 and PI3K/Akt/GSK3beta/NF-kappaB signalling axes and enhancing splenic Tregs in DSS-induced murine chronic colitis, Food Funct. 12 (18) (2021) 8492–8506.
[20] A.K. Farha, R.Y. Gan, H.B. Li, D.T. Wu, A.G. Atanasov, K. Gul, J.R. Zhang, Q.Q. Yang, H. Corke, The anticancer potential of the dietary polyphenol rutin: current status, challenges, and perspectives, Crit. Rev. Food Sci. Nutr. 62 (3) (2022) 832–859.
[21] A. Koh, F. De Vadder, P. Kovatcheva-Datchary, F. Backhed, From dietary fiber to host physiology: short-chain fatty acids as key bacterial metabolites, Cell 165 (6) (2016) 1332–1345.
[22] J. Hu, H. Huang, Y. Che, C. Ding, L. Zhang, Y. Wang, H. Hao, H. Shen, L. Cao, Qingchang Huashi Formula attenuates DSS-induced colitis in mice by restoring gut microbiota-metabolism homeostasis and goblet cell function, J. Ethnopharmacol. 266 (2021), 113394.
[23] J.H. Tao, J.A. Duan, W. Zhang, S. Jiang, J.M. Guo, D.D. Wei, Polysaccharides from Chrysanthemum morifolium ramat ameliorate colitis rats via regulation of the metabolic profiling and NF-kappa B/TLR4 and IL-6/JAK2/STAT3 signaling pathways, Front. Pharmacol. 9 (2018) 746.
[24] T. Xiong, X. Zheng, K. Zhang, H. Wu, Y. Dong, F. Zhou, B. Cheng, L. Li, W. Xu, J. Su, J. Huang, Z. Jiang, B. Li, B. Zhang, G. Lv, S. Chen, Ganluyin ameliorates DSS-induced ulcerative colitis by inhibiting the enteric-origin LPS/TLR4/NF-kappaB pathway, J. Ethnopharmacol. 289 (2022), 115001.
[25] H. Li, Y. Wang, S. Shao, H. Yu, D. Wang, C. Li, Q. Yuan, W. Liu, J. Cao, X. Wang, H. Guo, X. Wu, S. Wang, Rabdosia serra alleviates dextran sulfate sodium salt-induced colitis in mice through anti-inflammation, regulating Th17/Treg balance, maintaining intestinal barrier integrity, and modulating gut microbiota, J Pharm Anal 12 (6) (2022) 824–838.
[26] J. He, K.J. Guo, Q. Chen, Y.L. Wang, Jirimutu, Camel milk modulates the gut microbiota and has anti-inflammatory effects in a mouse model of colitis, J. Dairy Sci. 105 (5) (2022) 3782–3793.
[27] Y. Yang, M. Li, Q. Liu, Q. Zhao, J. Zeng, Q. Wang, Y. Zhao, F. Du, Y. Chen, J. Shen, H. Luo, S. Wang, W. Li, M. Chen, X. Li, F. Wang, Y. Sun, L. Gu, Z. Xiao, Y. Du, X. Wu, Starch from Pueraria lobata and the amylose fraction alleviates dextran sodium sulfate induced colitis in mice, Carbohydr. Polym. 302 (2023), 120329.
[28] H. Yao, Y. Shi, J. Yuan, R. Sa, W. Chen, X. Wan, Matrine protects against DSS-induced murine colitis by improving gut barrier integrity, inhibiting the PPAR-alpha signaling pathway, and modulating gut microbiota, Int. Immunopharm. 100 (2021), 108091.
[29] J. Chang, R.W. Leong, V.C. Wasinger, M. Ip, M. Yang, T.G. Phan, Impaired intestinal permeability contributes to ongoing bowel symptoms in patients with inflammatory bowel disease and mucosal healing, Gastroenterology 153 (3) (2017) 723–731 e721.
[30] H. Xiao, H. Li, Y. Wen, D. Jiang, S. Zhu, X. He, Q. Xiong, J. Gao, S. Hou, S. Huang, L. He, J. Liang, Tremella fuciformis polysaccharides ameliorated ulcerative colitis via inhibiting inflammation and enhancing intestinal epithelial barrier function, Int. J. Biol. Macromol. 180 (2021) 633–642.
[31] K. Kobayashi, K. Matsunaga, Y. Tsugami, H. Wakasa, T. Nishimura, IL-1beta is a key inflammatory cytokine that weakens lactation-specific tight junctions of mammary epithelial cells, Exp. Cell Res. 409 (2) (2021), 112938.
[32] X.Y. Cao, J.H. Ni, X. Wang, G.Z. Feng, H.D. Li, W.L. Bao, Y.R. Wang, K.Y. You, H.B. Weng, X.Y. Shen, Total glucosides of Paeony restores intestinal barrier function through inhibiting Lyn/Snail signaling pathway in colitis mice, Phytomedicine 87 (2021), 153590.
[33] M.R. Schneider, M. Dahlhoff, D. Horst, B. Hirschi, K. Trulzsch, J. Muller-Hocker, R. Vogelmann, M. Allgauer, M. Gerhard, S. Steininger, E. Wolf, F.T. Kolligs, A key role for E-cadherin in intestinal homeostasis and Paneth cell maturation, PLoS One 5 (12) (2010), e14325.
[34] X. Wang, S. Chen, H. Xiang, Z. Liang, H. Lu, Role of sphingosine-1-phosphate receptors in vascular injury of inflammatory bowel disease, J. Cell Mol. Med. 25 (6) (2021) 2740–2749.
[35] H. Nishimura, H. Fukui, X. Wang, N. Ebisutani, T. Nakanishi, T. Tomita, T. Oshima, S. Hirota, H. Miwa, Role of the beta-catenin/REG ialpha Axis in the proliferation of sessile serrated adenoma/polyps associated with fusobacterium nucleatum, Pathogens 10 (4) (2021).
[36] X. Yan, Y. Zhai, W. Zhou, Y. Qiao, L. Guan, H. Liu, J. Jiang, L. Peng, Intestinal flora mediates antiobesity effect of rutin in high-fat-diet mice, Mol. Nutr. Food Res. 66 (14) (2022), e2100948.

[37] H. Yang, R. Cai, Z. Kong, Y. Chen, C. Cheng, S. Qi, B. Gu, Teasaponin ameliorates murine colitis by regulating gut microbiota and suppressing the immune system response, Front. Med. 7 (2020), 584369.
[38] I. Mukhopadhya, R. Hansen, E.M. El-Omar, G.L. Hold, IBD-what role do Proteobacteria play? Nat. Rev. Gastroenterol. Hepatol. 9 (4) (2012) 219–230.
[39] X.Y. Zhang, J. Chen, K. Yi, L. Peng, J. Xie, X. Gou, T. Peng, L. Tang, Phlorizin ameliorates obesity-associated endotoxemia and insulin resistance in high-fat diet-fed mice by targeting the gut microbiota and intestinal barrier integrity, Gut Microb. 12 (1) (2020) 1–18.
[40] J. Jia, P. Zhang, C. Zhang, G. Jiang, W. Zheng, S. Song, C. Ai, Sulfated polysaccharides from pacific abalone attenuated DSS-induced acute and chronic ulcerative colitis in mice via regulating intestinal micro-ecology and the NF-kappaB pathway, Food Funct. 12 (22) (2021) 11351–11365.
[41] J.G. Lee, J. Lee, A.R. Lee, S.V. Jo, C.H. Park, D.S. Han, C.S. Eun, Impact of short-chain fatty acid supplementation on gut inflammation and microbiota composition in a murine colitis model, JNB (J. Nutr. Biochem.) 101 (2022), 108926.
[42] J. Ji, X. Ge, Y. Chen, B. Zhu, Q. Wu, J. Zhang, J. Shan, H. Cheng, L. Shi, Daphnetin ameliorates experimental colitis by modulating microbiota composition and T (reg)/T(h)17 balance, FASEB (Fed. Am. Soc. Exp. Biol.) J. 33 (8) (2019) 9308–9322.
[43] F. Wan, M. Wang, R. Zhong, L. Chen, H. Han, L. Liu, Y. Zhao, H. Lv, F. Hou, B. Yi, H. Zhang, Supplementation with Chinese medicinal plant extracts from Lonicera hypoglauca and scutellaria baicalensis mitigates colonic inflammation by regulating oxidative stress and gut microbiota in a colitis mouse model, Front. Cell. Infect. Microbiol. 11 (2021), 798052.
[44] C.J. Meehan, R.G. Beiko, A phylogenomic view of ecological specialization in the Lachnospiraceae, a family of digestive tract-associated bacteria, Genome Biology and Evolution 6 (3) (2014) 703–713.
[45] H. Huang, M. Li, Y. Wang, X. Wu, J. Shen, Z. Xiao, Y. Zhao, F. Du, Y. Chen, Z. Wu, H. Ji, C. Zhang, J. Li, Q. Wen, P.J. Kaboli, C.H. Cho, S. Wang, Y. Wang, Y. He, X. Wu, Excessive intake of longan arillus alters gut homeostasis and aggravates colitis in mice, Front. Pharmacol. 12 (2021), 640417.
[46] F. Dong, F. Xiao, X. Li, Y. Li, X. Wang, G. Yu, T. Zhang, Y. Wang, Pediococcus pentosaceus CECT 8330 protects DSS-induced colitis and regulates the intestinal microbiota and immune responses in mice, J. Transl. Med. 20 (1) (2022) 33.
[47] C. Martin-Gallausiaux, L. Marinelli, H.M. Blottiere, P. Larraufie, N. Lapaque, SCFA: mechanisms and functional importance in the gut, Proc. Nutr. Soc. 80 (1) (2021) 37–49.
[48] D. Ashley, D. Marasini, C. Brownmiller, J.A. Lee, F. Carbonero, S.O. Lee, Impact of grain sorghum polyphenols on microbiota of normal weight and overweight/obese subjects during in vitro fecal fermentation, Nutrients 11 (2) (2019).
[49] Z. Wu, S. Huang, T. Li, N. Li, D. Han, B. Zhang, Z.Z. Xu, S. Zhang, J. Pang, S. Wang, G. Zhang, J. Zhao, J. Wang, Gut microbiota from green tea polyphenol-dosed mice improves intestinal epithelial homeostasis and ameliorates experimental colitis, Microbiome 9 (1) (2021) 184.
[50] L. Ni, Q. Lu, M. Tang, L. Tao, H. Zhao, C. Zhang, Y. Yu, X. Wu, H. Liu, R. Cui, Periplaneta americana extract ameliorates dextran sulfate sodium-induced ulcerative colitis via immunoregulatory and PI3K/AKT/NF-kappaB signaling pathways, Inflammopharmacology 30 (3) (2022) 907–918.
[51] Q. Fan, X. Guan, Y. Hou, Y. Liu, W. Wei, X. Cai, Y. Zhang, G. Wang, X. Zheng, H. Hao, Paeoniflorin modulates gut microbial production of indole-3-lactate and epithelial autophagy to alleviate colitis in mice, Phytomedicine 79 (2020), 153345.
[52] S.J. Huang, S.P. Hu, S. Liu, B. Tang, Y.J. Liu, L. Tang, Y.Y. Lei, L. Zhong, S.M. Yang, S. He, Lithium carbonate alleviates colon inflammation through modulating gut microbiota and Treg cells in a GPR43-dependent manner, Pharmacol. Res. (2022) 175.

Abbreviations

UC: Ulcerative colitis
IBD: Inflammatory bowel disease
SCFAs: Short-chain fatty acids
LPS: Lipopolysaccharide;
TJ: tight junction
AJ: adherent junction
FMT: Fecal Microbial Transplantation
PGF: Pseudo-germ-free
Rut: Rutin
MDGP: Moutai distiller's grains polyphenol extract
LC-HR-ESI-MS: liquid chromatography-high-resolution electrospray ionization mass spectrometry